Boundary Effects on Multiplication Noise in Thin Heterostructure Avalanche Photodiodes: Theory and Experiment

Majeed M. Hayat, *Senior Member, IEEE*, Oh-Hyun Kwon, Shuling Wang, Joe C. Campbell, *Fellow, IEEE*, Bahaa E. A. Saleh, *Fellow, IEEE*, and Malvin C. Teich, *Fellow, IEEE*

Abstract—The history-dependent recurrence theory for multiplication noise in avalanche photodiodes (APDs), developed by Hayat *et al.*, is generalized to include inter-layer boundary effects in heterostructure APDs with multilayer multiplication regions. These boundary effects include the initial energy of injected carriers as well as bandgap-transition effects within a multilayer multiplication region. It is shown that the excess noise factor can be significantly reduced if the avalanche process is initiated with an energetic carrier, in which case the initial energy serves to reduce the initial dead space associated with the injected carrier. An excess noise factor reduction up to 40% below the traditional thin-APD limit is predicted for GaAs, depending on the operational gain and the multiplication-region's width. The generalized model also thoroughly characterizes the behavior of dead space as a function of position across layers. This simultaneously captures the effect of the nonuniform electric field as well as the anticipatory nature of inter-layer bandgap-boundary effects. Such anticipatory behavior of the dead space is ignored in simplified models where the dead space is assumed to change abruptly at the layer boundary. The theory is applied to recently fabricated thin $Al_{0.6}Ga_{0.4}As$/GaAs heterostructure APDs exhibiting low excess noise factors. The excess noise factor predictions are in very good agreement with experiment. In one device, where the initial-energy effect is pronounced, the measured excess noise factor is 36% below the value predicted by previous analytical multiplication models which ignore the initial-energy effect.

Index Terms—Bandgap-boundary effects, carrier injection, dead space, excess noise factor, heterostructure APDs, impact ionization, ionization threshold energy, thin APDs.

I. INTRODUCTION

RECENT increased demand for avalanche photodiodes (APDs) for long-haul and metropolitan optical networks has fueled a renewed interest in the design of novel APD structures that exhibit both low avalanche noise and high bandwidth. By now, it has become evident that a practical way to reduce both multiplication noise and avalanche buildup

time is by reducing the thickness of the APD's multiplication layer (e.g., below 400 nm), as has been demonstrated by many groups in the past few years [1]–[17]. The reduction of the excess noise factor in thin APDs is attributable to the dead-space effect, which results from the role of a carrier's past history on its ability to create a new carrier pair via impact ionization. A newly generated carrier is capable of causing an impact ionization only after it travels a sufficient distance, called the dead space, in the course of which it gains enough energy from the field to permit it to cause another impact ionization. The conventional avalanche multiplication model, first developed by McIntyre [18], does not account for the dead-space effect nor does it predict the reduction of the excess noise factor for thin APDs. The effect of dead space on the gain and excess noise factor has been extensively studied and modern multiplication models that take carriers' history into account have been developed and tested against experimental measurements [6]–[13], [19]–[26].

Recently, a new breed of heterostructure APDs have been demonstrated to exhibit excess-noise factors that are well below the predictions of the dead-space-inclusive multiplication models for thin APDs [27], [28]. Although it has been strongly believed that the reduction in the excess noise factor is a result of the heterostructure, no clear understanding exists for the reason for this behavior. In this paper, we show that a reduction beyond the traditional dead-space-based limit is possible in a heterostructure APD through the following mechanism. In certain structures, injected carriers enter the multiplication region with substantial kinetic energy, gained when they traverse a short-lived field gradient just before entering the multiplication region. Such an initial energy serves to reduce the *initial* dead space associated with the injected avalanche-initiating carrier. This, in turn, will enhance the likelihood that the injected carrier impact ionizes in the very onset of the multiplication process. To get a feel for why this initial-energy effect reduces gain uncertainty, consider the extreme case for which we assume that an injected electron can "immediately" impact ionize as it enters the multiplication layer. (Note that in this special case, there is no uncertainty in the location of the first impact ionization.) In this case, a straightforward calculation shows that based on an equal multiplication gain, g, comparison, the excess noise factor F is reduced by a factor $[1 + F_c(g/2)]/2F_c(g)$, where F_c corresponds to the conventional dead-space-modified excess noise factor in the absence of the initial energy of the injected

carrier.[1] For example, if we select $g = 20$ for a 1000-nm GaAs APD, the noise reduction factor is approximately 0.32. The noise reduction in the above hypothetical situation is merely the result of the fact that the location of the *first* impact ionization was assumed to be concentrated at the origin. In actuality, there will still be some uncertainty in the location of the first ionization even if the initial dead space is completely eliminated. Nonetheless, the mere reduction of the initial dead space will directly act to bias the location of the first ionization toward the origin.

There is yet a related mechanism, namely, the bandgap-boundary effect, that may also contribute to changing the noise characteristics in APDs with multilayered multiplication regions. In such heterostructures, a carrier traversing the multiplication region may encounter a sudden change in the ionization threshold energy as it crosses the boundary between layers within the multiplication region. For example, it is quite possible that a carrier that has not yet built up the ionization threshold energy for one material becomes immediately capable of ionizing as soon as it crosses over to the other layer (assuming that the second layer has a lower ionization threshold energy than the first layer). An opposite effect may occur for the other species, as they encounter an increase in the threshold energy. This will result in a reduction in the required dead space for one species in a certain locality of the layer's boundary while the dead space for the other species increases. Such anticipatory behavior of dead space (as the carrier approaches the boundary) may contribute in localizing the ionizations and may affect the excess noise factor. We emphasize that such possible ionization localization effect near the layer boundary is solely related to the dead-space effect through the abrupt change in the threshold energy at the layer boundary. In particular, we do not assume any localized change in the ionization coefficients as a result of bandedge discontinuity at the layer boundary beyond what is dictated by the type of material and the electric field. In fact, a recent Monte-Carlo study on $Al_{0.6}Ga_{0.4}As/GaAs$ multilayers showed that bandedge discontinuities in multilayer structures offer no ionization-coefficient enhancement due to carrier energy losses brought about by phonon scattering [29].

Interestingly, both initial-energy and bandgap-boundary effects have one thing in common. In both cases, some form of "built-up energy" is used to reduce the dead space at *specific* locations (i.e., either at the multiplication region edge or near the boundary of layers within the multiplication region), which will induce some level of localization in the ionization events. The difference between the two effects has to do with the cause of the change in the dead space. In the case of the bandgap-boundary effect, the dead space varies abruptly *near* locations where there are jumps in the ionization threshold. The bandgap-boundary effect has an anticipatory nature, which reflects the fact that a carrier's dead space at a particular location depends on whether or not the carrier will encounter a threshold jump in its future.

In this paper, we generalize the dead-space multiplication theory (DSMT) developed by Hayat *et al.* [22], [23] to include the injected-carrier's initial energy and the bandgap-boundary effect. The theory is used to predict the extent of the reduction in the excess noise factor and to establish the relationship between this noise reduction and the width of the multiplication layer. The theory is applied to three recently fabricated APDs.

II. IMPACT IONIZATION MODEL

In this section, we generalize the hard-threshold impact-ionization model for the distance between the carrier's successive ionizations, originally developed in [22] and [23], to include the bandgap-boundary effect. Consider a multiplication region extending from $x = 0$ to $x = w$, and assume that the electric field therein is $\mathcal{E}(x)$, pointing in the opposite direction. We will further assume, in general, that the multiplication region consists of multiple layers. The goal is to characterize the probability density function (pdf) of the distance from the birth location of a carrier to the location of its first impact ionization thereafter. Following the notation in [23], if an electron (respectively, hole) is born at position x, we let $h_e(\xi \mid x)$ [respectively, $h_h(\xi \mid x)$] denote the pdf of the distance to the first ionization, measured from the carrier's birth position at x. For example, $h_e(\xi \mid x)\Delta$ is approximately the probability that an electron born at x first impact ionizes somewhere in the interval $[x+\xi, x+\xi+\Delta]$. We begin by identifying the key physical parameters that govern this pdf. These are: 1) the multiplication-region's ionization threshold-energy profile; 2) the carrier's dead-space profile; and 3) the profile of the ionization coefficients of enabled carriers (those that have traveled the required dead space). To accommodate the requirement that the multiplication region may consist of layers of different materials, we will allow the electron and hole ionization threshold energies, $E_{ie}(x)$ and $E_{ih}(x)$, respectively, to be position-dependent.

For an electron (respectively, hole) created at position x, let $d_e(x)$ [respectively, $d_h(x)$] be the dead space with which it is associated. With this convention, an electron (respectively, hole) which is newly created at position x cannot impact ionize before reaching $x + d_e(x)$ [respectively, $x - d_h(x)$]. Finally, let α and β denote the electron and hole ionization coefficients, respectively, associated with carriers that have acquired the ionization threshold energy. The authors and others have lately developed a methodology to extract these ionization coefficients from noise-versus-gain data [6], [7]. These coefficients are material specific and depend only on the electric field $\mathcal{E}(x)$, independently of the multiplication-layer width. For example, the electron ionization coefficient is given by

$$\alpha(x) = A \exp[-(\mathcal{E}_c/\mathcal{E}(x))^m]. \tag{1}$$

The parameters for the above exponential model for GaAs (as well as $Al_{0.2}Ga_{0.8}As$, InP, and $In_{0.52}Al_{0.48}As$) are reported in [7] and will be used in this paper. For $Al_{0.6}Ga_{0.4}As$, on the other hand, the parameters used in this paper are those developed by Plimmer *et al.* [13] using a Monte-Carlo technique in conjunction with multiplication data. When the above model for the ionization coefficients is used in conjunction with the DSMT [22], [23], correct prediction of the excess noise factor, the breakdown

---

[1]To see this, we write the random gain G in the presence of the initial energy of the injected carrier as $G'_c + G''_c$, where G'_c and G''_c are independent and identically-distributed gains corresponding to the initial offspring pair of electrons (with no initial energy). Now, compute the first and second moments of G in terms of the respective quantities for G'_c and G''_c, and use the fact that $\langle G'_c \rangle = \langle G''_c \rangle = 0.5 \langle G \rangle$ and $F_c = \langle (G'_c)^2 \rangle / \langle G'_c \rangle^2 = \langle (G''_c)^2 \rangle / \langle G''_c \rangle^2$.

voltage, and the frequency response of a variety of III–V thin APDs is obtained [6]–[8], [16], [30].

The above probability densities can be easily modified to utilize the more realistic soft-threshold ionization models for which the newly created carriers gradually attain their ionization capability [17]. However, in this paper we chose to use the simplified hard-threshold dead-space model as an approximation. This model manages to capture the dead-space effect while keeping the mathematical complexity of the model to a minimum. It also alleviates the need for estimating the soft-threshold profile of the ionization densities, which is typically achieved by means of Monte-Carlo simulation.

In the subsections to follow, we will describe a procedure for calculating the position-dependent dead space in a multilayer multiplication region. With the availability of profiles of the dead-space and the ionization coefficients, the expression for $h_e(\xi \,|\, x)$ is given by [23]

$$h_e(\xi \,|\, x) = \begin{cases} \alpha(x+\xi)e^{-\int_{d_e(x)}^{\xi} \alpha(x+y)\,dy}, & \xi \geq d_e(x) \\ 0, & \xi < d_e(x) \end{cases} \quad (2)$$

and

$$h_h(\xi \,|\, x) = \begin{cases} \beta(x-\xi)e^{-\int_{d_h(x)}^{\xi} \beta(x-y)\,dy}, & \xi \geq d_h(x) \\ 0, & \xi < d_h(x) \end{cases}. \quad (3)$$

To make the above pdfs suitable for multilayer multiplication regions, we must thoroughly characterize the dead space profiles in heterostructures.

A. Characterization of Dead Space in Heterostructures

Under the simplifying assumption that after each impact ionization a carrier starts from zero initial energy, the minimum distance that an electron, born at position x, must travel before acquiring the ionization threshold energy is governed by the following energy relation:

$$q\int_{x}^{x+d_e(x)} \mathcal{E}(y)\,dy = E_{\text{ie}}(x+d_e(x)). \quad (4)$$

The above expression is a simple extension of the dead-space definition in [23], which now captures position-dependent ionization thresholds. Recall that the threshold energy $E_{\text{ie}}(x)$ may vary with x according to the type of material at x. Furthermore, observe that for each x, the relevant ionization threshold energy is the value at the point where the carrier attains the ionization threshold. Hence, for an electron born at location x, the dead space $d_e(x)$ which must be traveled, is the minimum nonnegative solution δ to the following equation:

$$q\int_{x}^{x+\delta} \mathcal{E}(y)\,dy = E_{\text{ie}}(x+\delta). \quad (5)$$

Similarly, the hole dead space $d_h(x)$ is the minimum nonnegative solution δ to the following equation:

$$q\int_{x-\delta}^{x} \mathcal{E}(y)\,dy = E_{\text{ih}}(x-\delta). \quad (6)$$

In our formulation of the dead-space model, we adopted the commonly-accepted assumption that the dead space is

deterministic. In actuality, the dead space is a random variable since a carrier may not necessarily loose all of its kinetic energy after each impact ionization. The extension of the pdfs of the carriers' free-path distance to capture this effect is straightforward. The trick is to first replace (2) and (3) by a conditional pdf (conditional on the actual realization of the random dead space) and then average over all possible realizations of the dead space. In the case of a uniform-field multiplication region, for example, if $f_{d_e}(\delta)$ is the pdf of the dead-space distance (in the hard dead space model), then an easy calculation shows that $h_e(x) = \alpha \exp(-\alpha x)\int_0^x \exp(\alpha\delta)f_{d_e}(\delta)\,d\delta$. The knowledge of $f_{d_e}(\delta)$ will ultimately depend on the knowledge of the energy probability distribution after impact ionization. We will not consider the stochastic dead space in our calculations in this paper since knowledge of the energy probability distribution is not presently available to us.

III. THE MODIFIED DEAD-SPACE MULTIPLICATION THEORY

In this section, we extend the DSMT recurrence theory [22], [23] to incorporate the initial energy of injected carriers gained prior to entering the multiplication region.

A. Preliminaries

We begin by briefly reviewing the DSMT developed in [23]. The theory involves recurrence equations for the electron- and hole-induced total offsprings $Z(x)$ and $Y(x)$, defined as the overall electron and hole progeny generated by a single parent electron (respectively, hole) at the position x in the multiplication region. In the case of electron injection at the edge of the multiplication region (at $x = 0$), the random gain G_{DSMT} of the APD is simply $(Z(0)+1)/2$. According to [23, eqs. (4) and (5)], the mean of $Z(x)$ and $Y(x)$, denoted by $z(x)$ and $y(x)$, obey the following set of coupled recurrence relations:

$$z(x) = \left[1 - \int_0^{w-x} h_e(\xi \,|\, x)\,d\xi\right]$$
$$+ \int_0^{w-x} [2z(x+\xi) + y(x+\xi)]h_e(\xi \,|\, x)\,d\xi \quad (7)$$

and

$$y(x) = \left[1 - \int_0^{x} h_h(\xi \,|\, x)\,d\xi\right]$$
$$+ \int_0^{x} [2y(x-\xi) + z(x-\xi)]h_h(\xi \,|\, x)\,d\xi. \quad (8)$$

The first term in (7) is the probability that an electron, born at x, does not impact ionize at all, and it simplifies to $\exp\{-\int_{d_e(x)}^{w-x} \alpha(x+\xi)\,d\xi\}$. Similarly, the first term in (8) simplifies to $\exp\{-\int_{d_h(x)}^{x} \beta(x-\xi)\,d\xi\}$.

The excess noise factor is given by

$$F_{\text{DSMT}} \equiv \frac{\langle G_{\text{DSMT}}^2 \rangle}{\langle G_{\text{DSMT}} \rangle^2} = \frac{z_2(0) + 2z(0) + 1}{[z(0) + 1]^2} \quad (9)$$

where $z_2(x) = \langle Z^2(x) \rangle$ and $y_2(x) = \langle Y^2(x) \rangle$ are the second moments of $Z(x)$ and $Y(x)$, respectively. According to [23, eqs.

(8) and (9)], these quantities are governed by the following pair of coupled recurrence relations:

$$z_2(x) = 1 - \int_0^{w-x} h_e(\xi \,|\, x)\, d\xi$$
$$+ \int_0^{w-x} [2z_2(x+\xi) + y_2(x+\xi)$$
$$+ 4z(x+\xi)y(x+\xi) + 2z^2(x+\xi)] h_e(\xi \,|\, x)\, d\xi \quad (10)$$

and

$$y_2(x) = 1 - \int_0^x h_h(\xi \,|\, x)\, d\xi$$
$$+ \int_0^x [2y_2(x-\xi) + z_2(x-\xi) + 4z(x-\xi)y(x-\xi)$$
$$+ 2y^2(x-\xi)] h_h(\xi \,|\, x)\, d\xi. \quad (11)$$

Clearly, the above formulation assumes that all carriers (including the injected carrier) start with zero initial energy. We will relax this condition in subsequent sections so that an injected carrier may have an arbitrary initial energy (and hence a different initial dead space).

B. Probability Density Function of the Initial Ionization Distance

In cases when the avalanche process is initiated with a carrier that has a finite initial energy, the energy that the parent carrier needs to build up before reaching the ionization threshold is reduced by an amount equal to the carrier's initial energy. Note that this one-time initial energy is acquired from the nonzero field just before entering the multiplication layer and can be approximated in a deterministic fashion using the electric field just before the multiplication region. (To be more realistic, the phonon energy loss must be deducted from the built-up energy.) If the initial energy acquired by an injected electron is E_0, then the initial dead space d_{e_0} is computed by solving the following modified dead-space equation. Find the minimum nonnegative δ for which

$$q \int_x^{x+\delta} \mathcal{E}(y)\, dy = E_{ie} - E_0 \quad (12)$$

where E_{ie} is the ionization threshold energy associated with the multiplication layer into which the parent carrier is injected. Clearly, if $E_0 \geq E_{ie}$, we set $d_{e_0} = 0$. Moreover, the pdf of the distance to the first impact ionization for this parent carrier is

$$h_{e_0}(\xi) = \begin{cases} \alpha(\xi) e^{-\int_{d_{e_0}}^{\xi} \alpha(y)\, dy}, & \xi \geq d_{e_0} \\ 0, & \xi < d_{e_0}. \end{cases} \quad (13)$$

In actuality the width of the pdf beyond the dead space is expected to be reduced as the initial energy increases. However, in the above expression we assumed that the shape of the pdf beyond the initial dead space is independent of the dead-space reduction (i.e., we only modified the dead space). This is done as an approximation since the dependence of the width of the pdf (beyond the dead space) on the initial energy is not analytically known to us at this point.

We emphasize that the distance between subsequent impact ionizations for the parent electron, on the other hand, is governed by (2). The key question is how to incorporate this initial dead-space concept into the DSMT recurrence technique. This question is addressed next.

C. Modified Recurrence Relations

Let $Z_0(x)$ be defined as $Z(x)$ with the exception that for the parent electron at x, the distance ξ to the first impact ionization has a pdf $h_{e_0}(\xi)$. The key observation here is that upon the first ionization of the injected electron, the two newly created electrons and hole will have zero initial energy, independently of the initial energy of their parent electron. Consequently, conditional on the initial ionization occurring at ξ, two independent copies of $Z(\xi)$ and one copy of $Y(\xi)$ are generated. Now by averaging over all possibilities for ξ, we obtain the following equation for the mean value $z_0(x) = \langle Z_0(x) \rangle$:

$$z_0(x) = 1 - \int_0^{w-x} h_{e_0}(\xi)\, d\xi$$
$$+ \int_0^{w-x} [2z(x+\xi) + y(x+\xi)] h_{e_0}(\xi \,|\, x)\, d\xi. \quad (14)$$

Similarly, we obtain the following equation for the second moment $z_{02}(x) = \langle Z_0^2(x) \rangle$:

$$z_{02}(x) = 1 - \int_0^{w-x} h_{e_0}(\xi)\, d\xi$$
$$+ \int_0^{w-x} [2z_2(x+\xi) + y_2(x+\xi)$$
$$+ 4z(x+\xi)y(x+\xi) + 2z^2(x+\xi)] h_{e_0}(\xi \,|\, x)\, d\xi. \quad (15)$$

Equations (14) and (15) establish the link between the multiplication process with an arbitrary pdf for the initial-ionization distance and the ordinary dead-space-based multiplication process for which there is no distinction between the pdf of the initial ionization and that corresponding to the subsequent ones. We call the totality of the DSMT recurrence model with the addition of the complementary relations (14) and (15) [including the definitions (12) and (13)] the modified dead-space multiplication theory (MDSMT).

Clearly, the MDSMT is a two-step calculation. First, (7), (8), (10), and (11) are solved (as done in the traditional DSMT, using an iterative technique, for instance). Second, the complementary equations (14) and (15) are executed, utilizing the pdf of the ionization distance of the initial carrier. Note that the second step is a one-shot calculation. The gain and excess noise factors are calculated using $\langle G_{\text{MDSMT}} \rangle = 0.5[1 + z_0(0)]$ and $F_{\text{MDSMT}} = (z_{02}(0) + 2z_0(0) + 1)/(z_0(0) + 1)^2$, respectively.

D. Excess Noise Reduction

To see the extent of the role played by the injected-carrier's initial energy on the excess noise factor, we computed the gain versus noise characteristics for GaAs under two models.

1) We first used the DSMT model, in which case the initial energy of injected carriers is assumed zero.
2) We then repeated the excess-noise calculations using the maximal-MDSMT model, in which case we assumed that the initial energy of the injected carrier is equal to the ion-
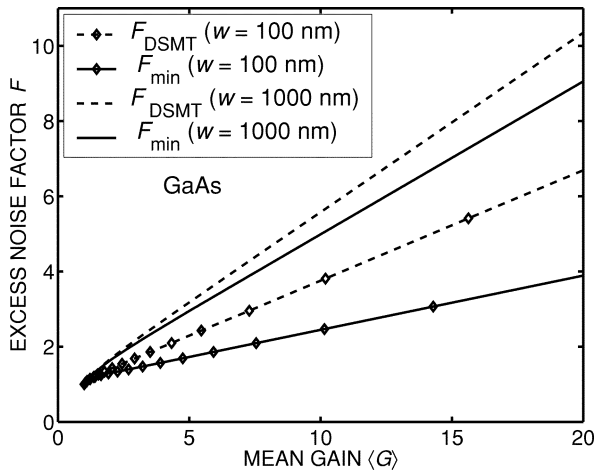
Fig. 1. Excess noise factor as a function of the mean gain for two GaAs APDs with multiplication-region widths of 100 nm (curves with diamonds) and 1000 nm. The solid curves represent the maximal MDSMT prediction $F_{\min}$ for which the initial energy is set to the ionization threshold energy (i.e., zero initial dead space for the injected electron). The dashed curves are the DSMT predictions F_{DSMT}.
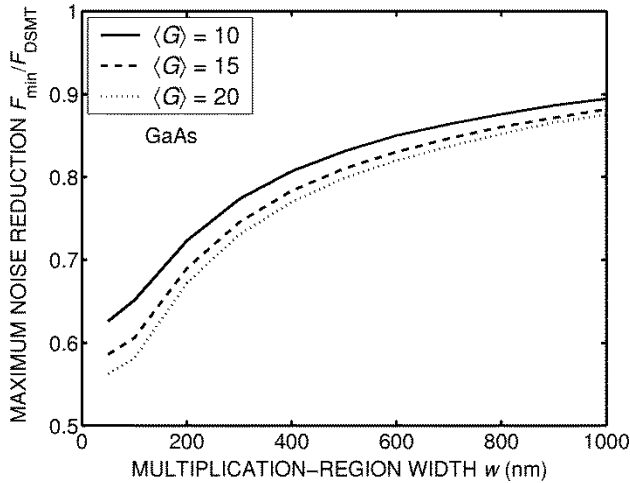

Fig. 2. Maximum possible reduction in the excess noise factor $F_{\min}/F_{\mathrm{DSMT}}$ as a function of the multiplication-region width for GaAs. The mean gain is used as a parameter.

ization threshold energy. This assumption forces the initial dead space of the injected carrier to vanish (without altering the shape of the pdf), and it represents the maximal initial-energy effect. We denote the excess noise factor under this assumption by $F_{\min}$, as the excess noise will be minimal. Fig. 1 depicts both F_{DSMT} and $F_{\min}$ for two widths, namely, $w = 100$ nm and $w = 1000$ nm. It is seen that the maximum reduction in the excess noise factor is more significant in the thin multiplication layer than the thick one. This is expected since the initial-energy effect plays its role through the dead-space effect, which is known to have a more significant impact on noise in thin multiplication layers. This behavior is more clearly seen in Fig. 2, where the maximal excess-noise-reduction factor $F_{\min}/F_{\mathrm{DSMT}}$ is plotted as a function of w for three gain values. We emphasize that the conclusion drawn from Fig. 2 regarding the width holds for the *maximum* excess-noise reduction possible, and it does not imply that an actual thin device necessarily exhibits
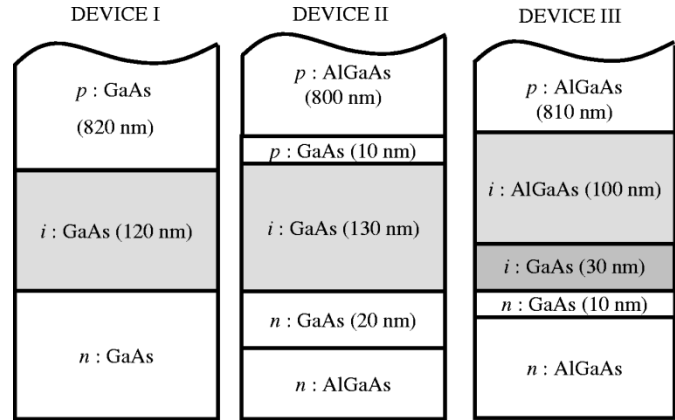

Fig. 3. Structure of the three APDs considered in this paper. Device I is a homostructure GaAs APD and it is used as a reference. Devices II and III are $Al_{0.6}Ga_{0.4}As$/GaAs heterostructure APDs, and the latter has a two-layer $Al_{0.6}Ga_{0.4}As$/GaAs multiplication region. Shaded areas represent the multiplication regions. Electrons are injected into the multiplication region from the top.

this effect more profoundly than a thick device. An added feature seen from Figs. 1 and 2 is that the maximum excess-noise reduction is higher at higher operational gains. This latter characteristic may be potentially useful in lowering receiver sensitivity as it will tend to elevate the optimal operational APD gain. Recall from Section 1 that the maximum excess-noise-factor reduction possible for a 1000-nm GaAs at a gain of 20 (with the unrealistic assumption of a delta-function pdf at the edge of the multiplication region) is 0.32, which is greater than the maximum reduction of 0.85 shown in Fig. 2. However, we note that $F_{\min}$ in Figs. 1 and 2 is calculated using zero initial dead space without altering the shape of the pdf after the dead space (i.e., no delta-function is assumed at the edge of the multiplication region). Thus, the predicted noise in Figs. 1 and 2 is greater than that predicted when ionization at the edge occurs with certainty.

IV. APPLICATION TO EXPERIMENTS

We now apply the theory to three devices, which are schematically shown in Fig. 3: Device I is a homojunction GaAs APD with $w = 120$ nm; Device II is a GaAs/$Al_{0.6}Ga_{0.4}As$ heterostructure APD, where the multiplication is confined to the GaAs layer and $w = 130$ nm; and Device III is GaAs/$Al_{0.6}Ga_{0.4}As$ heterostructure APD, for which the multiplication takes place in both (adjacent) $Al_{0.6}Ga_{0.4}As$ (100 nm) and GaAs (30 nm) layers. The width of the overall multiplication region for Device III is thus 130 nm.[2] (The structural and fabrication details of these devices, beyond what is included in this paper, will be reported elsewhere.) Devices II and III are the devices of most interest in this paper, while Device I is used here as a reference. Figs. 4 and 5 show the electric field profiles for Devices II and III, respectively, parameterized by the applied reverse-bias voltage. The electric fields were calculated using MEDICI software according to the doping profiles obtained from secondary ion mass spectroscopy (SIMS).

[2]These devices were fabricated and tested at the Microelectronics Research Center at the University of Texas in Austin.
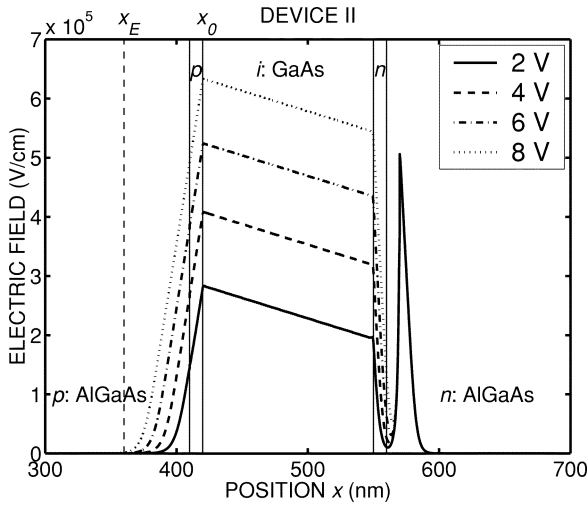
Fig. 4. Electric field profile for Device II. Solid vertical lines represent layer boundaries, and the dashed vertical line is used to illustrate the location x_E of the onset of the field buildup. The point x_0 marks the start of the multiplication layer. The fields were calculated using MEDICI software according to the doping profiles obtained from SIMS data. Notice the extent of the spread of the field gradient to the left of the i-layer.
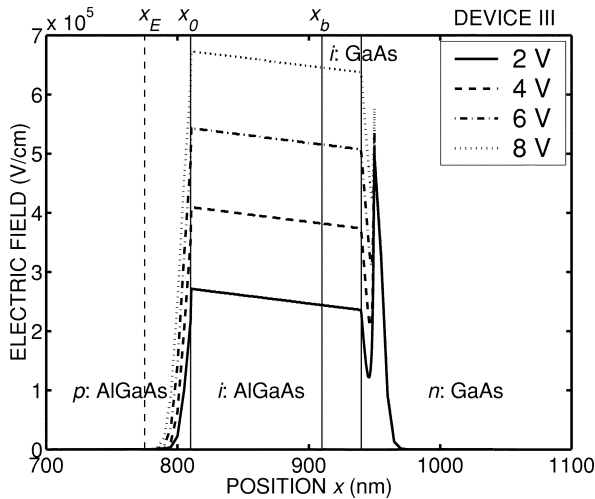

Fig. 5. Same as Fig. 4, but for Device III. This structure has two multiplication layers, namely, $Al_{0.6}Ga_{0.4}As$ and GaAs.

A. Dead-Space Profile

The dead-space profiles in the i-layers for Devices I and II were calculated using the fact that the field is linear in the i-layers. An analytical solution to (5) and (6) was obtained, involving the voltage-dependent parameters that comprise the linear electric-field profile. For Devices I and II, the multiplication region consists of a single GaAs layer, and as expected, calculations show that the dead space slightly increases with x as the field decreases. In the case of Device I, electron and hole normalized dead spaces (d/w) are approximately 0.21 and 0.17, respectively, and the corresponding values for Device II are 0.25 and 0.20, respectively, for electrons and holes.

The dead-space behavior is more complex for Device III (as shown in Fig. 6) for which the threshold energy changes abruptly at the $Al_{0.6}Ga_{0.4}As$/GaAs boundary point marked x_b in Fig. 6. At x_b, the threshold changes from
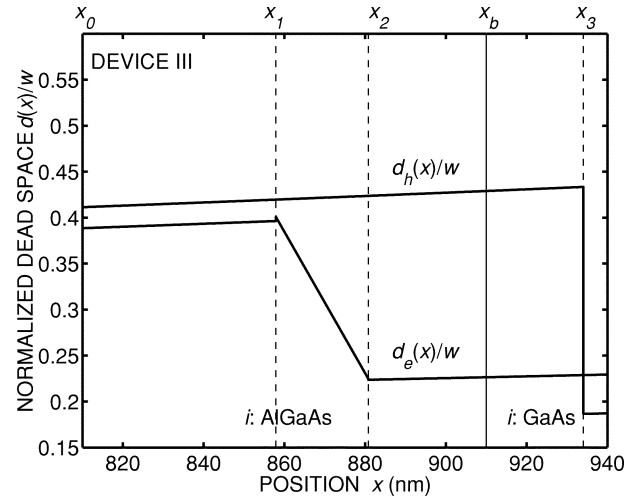

Fig. 6. Electron and hole dead-space profiles in the multiplication layers for Device III. The solid vertical line represents the $Al_{0.6}Ga_{0.4}As$/GaAs boundary.

$E_{ie,AlGaAs} = 3.4$ eV to $E_{ie,GaAs} = 1.90$ eV for electrons, and from $E_{ih,GaAs} = 1.55$ eV to $E_{ih,AlGaAs} = 3.6$ eV for holes. We will examine the electron dead space first. Referring to Fig. 6, we first define x_1 as the point that is exactly one electron dead-space to the left of the boundary, i.e., x_1 has the property $x_1 + d_e(x_1) = x_b$. Hence, if an electron is born to the left of x_1, then it will complete the required dead space within the $Al_{0.6}Ga_{0.4}As$ layer (i.e., $d_e(x) + x < x_b$). Thus, for $x < x_1, d_e(x)$ is the solution to $q \int_x^{x+\delta} \mathcal{E}(y)\,dy = E_{ie,AlGaAs}$. On the other hand, if an electron is born to the right of x_1, then it will complete the required dead space once it is in the GaAs layer (i.e., $d_e(x) + x > x_b$ and $d_e(x)$ is the solution to $q \int_x^{x+\delta} \mathcal{E}(y)\,dy = E_{ie,GaAs}$). Now x_2 is defined as the point for which the electron energy, accumulated from x_2 to x_b, is exactly equal to $E_{ie,GaAs}$. Thus, if an electron is born in the range $x_1 < x < x_2$, then by the time it reaches the boundary point x_b it will have already acquired the ionization threshold for GaAs. Consequently, for $x_1 < x < x_2, d_e(x) = x_b - x$, and this is the reason for the abrupt change in the graph of $d_e(x)$ to a negative slope at $x = x_1$. Finally, when an electron is born to the right of x_2, then it must travel a further distance (beyond the boundary point) in GaAs before accumulating the threshold energy $E_{ie,GaAs}$, and the dead space increases gradually thereafter as a result of the linear decrease in the field. In summary, the abrupt change in the threshold energy at the boundary brings about a steep transition in the dead space at $x = x_1$, which occurs well before the layer boundary x_b. This is a manifestation of the anticipatory behavior of dead space prior to the layer boundary.

The situation is somewhat different for holes as, unlike electrons, they experience an upward transition in the ionization threshold energy as they cross the material boundary at x_b from right to left. Referring again to Fig. 6, we define the point x_3 with the property $x_3 - d_h(x_3) = x_b$ (i.e., $q \int_{x_b}^{x_3} \mathcal{E}(y)\,dy = E_{ih,GaAs}$). Thus, if a hole is born to the left of x_3, then it will complete traveling the required dead space only after it is inside the $Al_{0.6}Ga_{0.4}As$ layer. In particular, for $x = x_3$, the energy that the hole acquires by the time it reaches the GaAs/$Al_{0.6}Ga_{0.4}As$
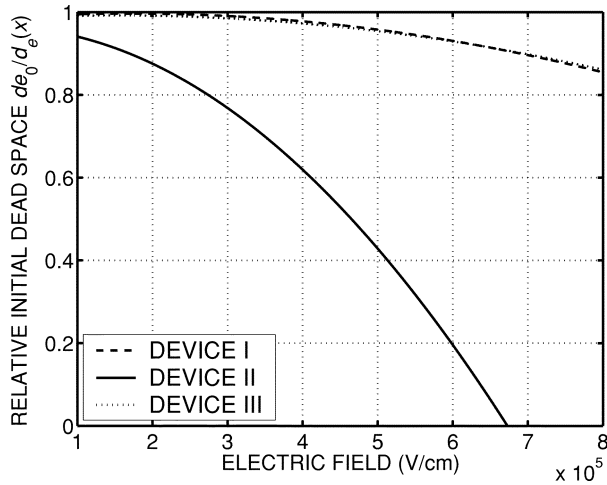
Fig. 7. Ratio of the injected electron's initial dead space d_{e_0} to the dead space in the absence of any initial energy $d_e(0)$ as a function of the average electric field in the multiplication region. Note that an injected carrier in Device II exhibits a significant reduction in the initial dead space from the customary (zero initial-energy) dead space, especially at high fields. In contrast, such a reduction is minimal in Devices I and III.
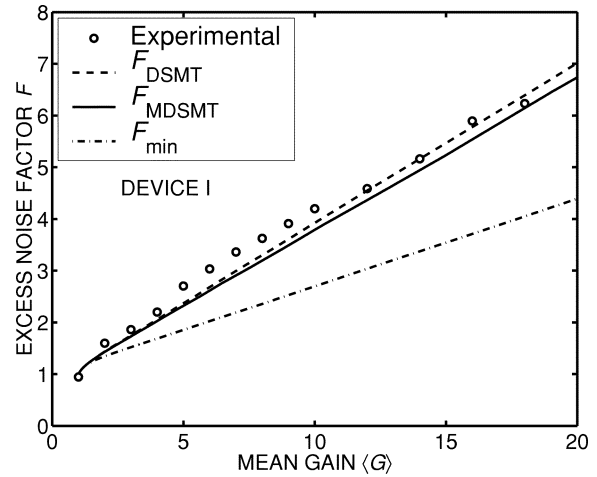

Fig. 8. Excess noise factor as a function of the mean gain for Device I. Circles represent measured values and the solid curve represents the MDSMT prediction F_{MDSMT}. For reference, the DSMT predictions F_{DSMT} (which assume zero initial energy for the injected carrier), and the maximal-MDSMT predictions F_{min} (for which the initial energy is set to the ionization threshold energy) are shown by the dashed-dotted and dashed curves, respectively. Since the initial energy of the injected electron is small in this device, both DSMT and MDSMT accurately predict the experimental data.

boundary at x_b is short of $E_{\mathrm{ih,AlGaAs}}$ by exactly 2.05 eV, and it must travel a further distance inside $\mathrm{Al_{0.6}Ga_{0.4}As}$ before accumulating a total energy of $E_{\mathrm{ih,AlGaAs}}$. This is the cause of the large upward jump in the graph of $d_h(x)$ at $x = x_3$, which is again a manifestation of the anticipatory behavior of the dead space.

We next use the above dead space profiles along with the initial-energy effect in conjunction with the MDSMT to predict the excess noise factor for the three devices.

B. Excess Noise Factor

To have a good initial feel for the magnitude of the initial dead space in each of the three devices, we computed the ratio of the injected-electron's initial dead space d_{e_0} to the customary dead space $d_e(0)$ at the edge of the multiplication region. To do so, the initial energy E_0 (in electronvolts) of the injected electron was calculated by integrating the electric field just before the multiplication layer, from x_E to x_0, as shown in Figs. 4 and 5. For each device, E_0 was calculated as a function of the applied reverse-bias voltage. (A parametric model, not shown here, for the electric field prior to the multiplication, from x_E to x_0, was derived and used to compute E_0 as a function of the reverse-bias voltage.) The quantities d_{e_0} and $d_e(0)$ were then calculated using (12) and (5), respectively, and their ratio was plotted as a function of the spatial average of the electric field in the multiplication region, as shown in Fig. 7. For Device II, $d_{e_0}/d_e(0)$ is expected to decrease to zero when the average field is 6.7 kV/cm, in which case the initial energy acquired by the injected carrier equates $E_{\mathrm{ie,GaAs}}$. In contrast, it is seen that for Devices I and III, the initial dead space remains within 10% of the ordinary dead space within the operational range of the electric field. This is a direct consequence of the contrast in the nature of the electric-field buildup in the p region just to the left of the multiplication region in Device II and Devices I and III.

In light of Fig. 7, we would expect that the role played by the initial-energy effect in carrier multiplication would be most
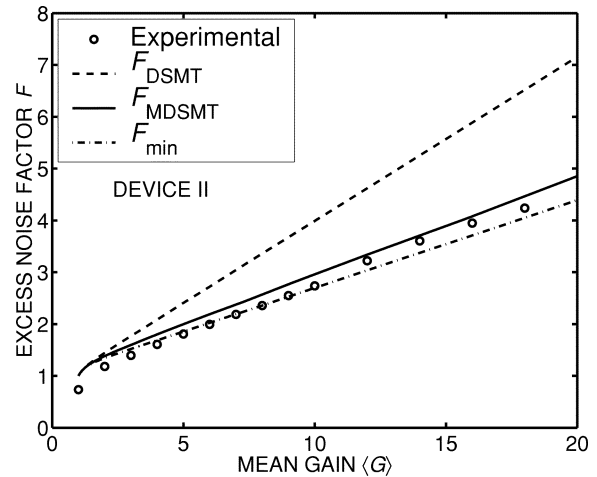

Fig. 9. Same as Fig. 8, but for Device II. The MDSMT model provides excellent agreement with the experimental data, while the DSMT model significantly overestimates the excess noise factor as a result of ignoring the initial energy of the injected electron.

significant in Device II, and far less significant in Devices I and III. Indeed, the MDSMT predicts just that, as shown in Figs. 8–10. We particularly note that the MDSMT accurately predicts the low excess noise factor in Device II, whereas the DSMT (in which the initial energy is ignored) overestimates the noise by approximately 45% in comparison with measured data (at $\langle G \rangle = 20$). Moreover, the reduction in the excess noise factor is near its maximal level for Device II, as seen by comparing the F_{min} and F_{MDSMT} curves, and the significant reduction in the noise is primarily a result of the initial-energy effect. For Device I, on the other hand, the discrepancy between the DSMT and the MDSMT is small ($<4\%$), and both models represent the data closely. This is because the initial-energy buildup in Device I is negligible relative to the ionization threshold energy. Similarly, the discrepancy between the DSMT and the MDSMT is
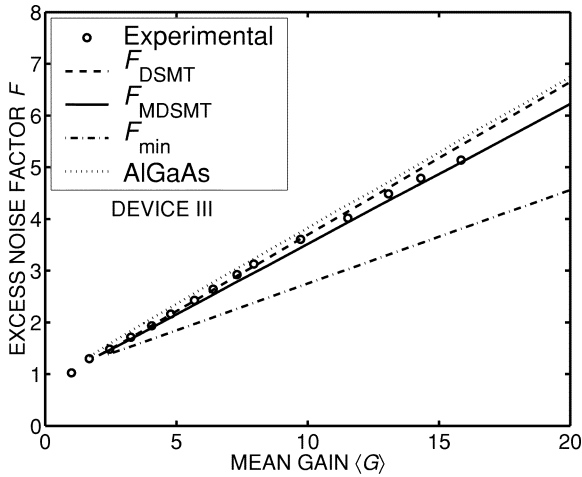
Fig. 10. Same as Fig. 8, but for Device III. As a result of the small initial energy, the discrepancy between the MDSMT and the DSMT predictions is small. The dotted line represents the MDSMT prediction for a hypothetical version of Device III for which both multiplication layers are $Al_{0.6}Ga_{0.4}As$. Ionization threshold energies for $Al_{0.6}Ga_{0.4}As$ and the ionization-coefficients parameters were taken from [13].

within 7% in Device III, as the initial-energy buildup is once again small, and the MDSMT approximates the data very well. The small error between the MDSMT predictions and the data in Devices I and III is most probably attributable to the fact that the parameters of the ionization-coefficient model for GaAs and $Al_{0.6}Ga_{0.4}As$ were extracted using models that ignored the initial-energy effect. In actuality, it is very likely that the devices that generated the data used in the model fitting exhibited a weak form of field gradient in the p-layer. Thus, the ionization coefficients for GaAs and $Al_{0.6}Ga_{0.4}As$ inherently capture a small level of the initial-energy effect. In order to exclude the role of the initial energy from the ionization coefficients, the initial-energy-effect should be included, in conjunction with the MDSMT, in future model fittings which render the ionization coefficients for various materials. The resulting ionization coefficients will then be truly material specific and independent of both the layer thickness and the initial energy of injected carriers.

To examine the role of the bandgap-boundary effect within the two-layer multiplication region in Device III, we repeated the gain-noise calculation, according to the MDSMT model, but with the simplistic assumption that the dead space changes abruptly at the layer boundary x_b. This action clearly ignores the bandgap-boundary-induced anticipatory nature of the electron and hole dead-space profiles depicted in Fig. 6. However, the excess noise factors obtained under this assumption (not shown) are approximately 5% higher than the MDSMT prediction shown in Fig. 10, which used the correct dead-space profile shown in Fig. 6. For comparison, we also generated the MDSMT predictions for a hypothetical version of Device III for which both multiplication layers are $Al_{0.6}Ga_{0.4}As$ (the same injected-carrier initial energy was assumed as in Device III). From Fig. 10 we see that F_{MDSMT} is approximately 8.5% lower than the excess noise factor for the single multiplication-layer $Al_{0.6}Ga_{0.4}As$ APD (shown as a dotted curve). We therefore conclude that the bandgap-boundary effect is not very strong

in this particular device. However, we suspect that this reduction can be further intensified by optimizing the widths of the individual layers within the multiplication region. In general, we believe that the ultra-low-noise characteristics of more elaborate heterostructure APDs [28] may be attributed in part to a combination of carrier initial energy, bandgap-boundary effects, proper selection of the widths of layers, and effective bandgap engineering.

Throughout the calculation of the initial energy, losses due to phonon scattering were ignored. To have an assessment of the magnitude of this loss, let us consider Device II, for which the initial-energy effect was high, and compute the average energy loss in the p-type $Al_{0.6}Ga_{0.4}As$. We take the total phonon scattering distance (segment of the p region over which the field gradient exists) as approximately 40 nm (see Fig. 4). Furthermore, as an approximation, we take the phonon scattering mean free path λ_e and the phonon energy $\hbar\omega$ from Chia et al. [29] (for 45% Al concentration) as 4 nm and 32.5 meV, respectively. With these estimates at hand, we estimate the total phonon loss in the p region in the vicinity of the GaAs i-layer as approximately 0.325 eV, which is approximately 17% of the initial energy when the mean gain is 20. Accounting for such a phonon loss will therefore reduce the initial-energy effect and the predicted excess noise factor is expected to be slightly higher than that shown in Fig. 9.

Another approximation used in our calculations for Device II was that secondary holes are not allowed to ionize in the p-type $Al_{0.6}Ga_{0.4}As$ layer, just before the i-type GaAs layer. Although such an ionization is theoretically possible, we expect that its probability is extremely small because holes entering the $Al_{0.6}Ga_{0.4}As$ layer will encounter a sudden increase in the ionization threshold (from 1.55 eV to 3.6 eV). Thus, in order for a hole to impact ionize, it must gain a net energy of 2.05 eV from the field gradient in the p-type layer. This is improbable as our calculations show that the maximum initial energy (at the highest measured reverse bias) that can be built up in Device II is no more than 1.7 eV.

We finally point out that we have discovered that including the mild nonuniform nature of the electric field in the calculations was not critical at all for the devices considered in this paper. Excellent accuracy can be achieved by adopting the constant-field assumption, which reduces the computational complexity significantly.

V. CONCLUSION

A number of thin heterostructure APDs have been lately developed and shown to exhibit excess noise factors that are well below the predictions rendered by state-of-the-art analytical avalanche multiplication models. Existing analytical multiplication models, including the DSMT, all assume a single multiplication layer, and more importantly, they ignore layer-boundary effects such as the effect of the initial energy of injected carriers and the boundary-bandgap effect. For example, ignoring the initial carrier energy of an injected carrier is convenient from a modeling perspective, as it simplifies the analysis by imposing that all carriers, including the injected

carrier, impact ionize according to a common probability law. However, if an injected carrier has an initial energy comparable to the ionization threshold energy, then this is shown to cause a significant reduction in the excess noise factor (e.g., a reduction of 36% at a gain of 20 for a 100-nm GaAs multiplication layer). In this paper, we have generalized the DSMT recurrence technique to account for boundary effects such as the initial energy of injected carriers and to accommodate multiple multiplication layers. The effect of bandgap boundary on the dead-space profile is also thoroughly characterized taking into account the anticipatory nature of the dead space relative to the material boundary. The generalized model was applied to three APDs and very good agreement with data was achieved, whereas in the case when the initial-energy effect was significant (as in Device II), the DSMT could not account for the data.

Finally, a type of APDs that inherently has a mechanism for building up carrier initial-energy is the separate-absorption-charge-multiplication (SACM) structure [15]. In the SACM structure, photo-generated carriers are generated in a low field absorption layer and travel through a charge layer with a linear field gradient before entering the multiplication region. The charge layer can therefore affect the excess noise as it may energize carriers before they enter the multiplication region. However, close attention must be given to the width of the charge layer as it not only governs the amount of initial energy but also the significance of any phonon scattering effects, which may result in losses in the initial energy.

REFERENCES

[1] G. S. Kinsey, C. C. Hansing, A. L. Holmes, Jr., B. G. Streetman, J. C. Campbell, and A. G. Dentai, "Waveguide $In_{0.53}Ga_{0.47}As$-$In_{0.52}Al_{0.48}As$ avalanche photodiode," *IEEE Photon. Technol. Lett.*, vol. 12, pp. 416–418, 2000.

[2] G. S. Kinsey, J. C. Campbell, and A. G. Dentai, "Waveguide avalanche photodiode operating at 1.55 μm with a gain-bandwidth product of 320 GHz," *IEEE Photon. Technol. Lett.*, vol. 13, pp. 842–844, 2001.

[3] C. Lenox, H. Nie, P. Yuan, G. Kinsey, A. L. Holmes, Jr., B. G. Streetman, and J. C. Campbell, "Resonant-cavity InGaAs-InAlAs avalanche photodiodes with gain-bandwidth product of 290 GHz," *IEEE Photon. Technol. Lett.*, vol. 11, pp. 1162–1164, 1999.

[4] P. Yuan, O. Baklenov, H. Nie, A. L. Holmes, Jr., B. G. Streetman, and J. C. Campbell, "High-speed and low-noise avalanche photodiode operating at 1.06 μm," *IEEE J. Select. Topics Quantum Electron.*, vol. 6, pp. 422–425, 2000.

[5] C. Hu, K. A. Anselm, B. G. Streetman, and J. C. Campbell, "Noise characteristics of thin multiplication region GaAs avalanche photodiodes," *Appl. Phys. Lett.*, vol. 69, pp. 3734–3736, 1996.

[6] P. Yuan, C. C. Hansing, K. A. Anselm, C. V. Lenox, H. Nie, A. L. Holmes, Jr., B. G. Streetman, and J. C. Campbell, "Impact ionization characteristics of III–V semiconductors for a wide range of multiplication region thicknesses," *IEEE J. Quantum Electron.*, vol. 36, pp. 198–204, 2000.

[7] M. A. Saleh, M. M. Hayat, P. Sotirelis, A. L. Holmes, Jr., J. C. Campbell, B. E. A. Saleh, and M. C. Teich, "Impact-ionization and noise characteristics of thin III–V avalanche photodiodes," *IEEE Trans. Electron Devices*, vol. 48, pp. 2722–2731, Dec. 2001.

[8] M. A. Saleh, M. M. Hayat, O.-H. Kwon, A. L. Holmes, Jr., J. C. Campbell, B. E. A. Saleh, and M. C. Teich, "Breakdown voltage in thin III–V avalanche photodiodes," *Appl. Phys. Lett.*, vol. 79, pp. 4037–4039, 2001.

[9] M. A. Saleh, M. M. Hayat, B. E. A. Saleh, and M. C. Teich, "Dead-space-based theory correctly predicts excess noise factor for thin GaAs and AlGaAs avalanche photodiodes," *IEEE Trans. Electron Devices*, vol. 47, pp. 625–633, 2000.

[10] P. Yuan, K. A. Anselm, C. Hu, H. Nie, C. Lenox, A. L. Holmes, Jr., B. G. Streetman, J. C. Campbell, and R. J. McIntyre, "A new look at impact ionization—Part II: Gain and noise in short avalanche photodiodes," *IEEE Trans. Electron Devices*, vol. 46, pp. 1632–1639, Aug. 1999.

[11] K. F. Li, D. S. Ong, J. P. R. David, G. J. Rees, R. C. Tozer, P. N. Robson, and R. Grey, "Avalanche multiplication noise characteristics in thin GaAs p^+-i-n^+ diodes," *IEEE Trans. Electron Devices*, vol. 45, pp. 2102–2107, Nov. 1998.

[12] D. S. Ong, K. F. Li, G. J. Rees, G. M. Dunn, J. P. R. David, and P. N. Robson, "A Monte Carlo investigation of multiplication noise in thin p^+-i-n^+ GaAs avalanche photodiodes," *IEEE Trans. Electron Devices*, vol. 45, pp. 1804–1810, Oct. 1998.

[13] S. A. Plimmer, J. P. R. David, R. Grey, and G. J. Rees, "Avalanche multiplication in $Al_xGa_{1-x}As$ ($x = 0$ to 0.60)," *IEEE Trans. Electron Devices*, vol. 47, pp. 1089–1097, 2000.

[14] H. Nie, K. A. Anselm, C. Lenox, P. Yuan, C. Hu, G. Kinsey, B. G. Streetman, and J. C. Campbell, "Resonant-cavity separate absorption, charge, and multiplication avalanche photodiodes with high-speed and high gain-bandwidth product," *IEEE Photon. Technol. Lett.*, vol. 10, pp. 409–411, 1998.

[15] K. A. Anselm, H. Nie, C. Hu, C. Lenox, P. Yuan, G. Kinsey, J. C. Campbell, and B. G. Streetman, "Performance of thin separate absorption, charge, and multiplication avalanche photodiodes," *IEEE J. Quantum Electron.*, vol. 34, pp. 482–490, 1998.

[16] C. H. Tan, J. P. R. David, S. A. Plimmer, G. J. Rees, R. C. Tozer, and R. Grey, "Low multiplication noise thin $Al_{0.6}Ga_{0.4}As$ avalanche photodiodes," *IEEE Trans. Electron Devices*, vol. 48, pp. 1310–1317, July 2001.

[17] C. H. Tan, J. P. R. David, G. J. Rees, and R. C. Tozer, "Treatment of soft-threshold in impact ionization," *J. Appl. Phys.*, vol. 90, pp. 2538–2543, 2001.

[18] R. J. McIntyre, "Multiplication noise in uniform avalanche photodiodes," *IEEE Trans. Electron Devices*, vol. ED-13, pp. 164–168, 1966.

[19] Y. Okuto and C. R. Crowell, "Ionization coefficients in semiconductors: A nonlocalized property," *Phys. Rev. B, Condens. Matter*, vol. 10, pp. 4284–2623, 1974.

[20] R. A. La Violette and M. C. Stapelbroek, "A non-Markovian model of avalanche gain statistics for solid-state photomultiplier," *J. Appl. Phys.*, vol. 65, pp. 830–836, 1989.

[21] B. E. A. Saleh, M. M. Hayat, and M. C. Teich, "Effect of dead space on the excess noise factor and time response of avalanche photodiodes," *IEEE Trans. Electron Devices*, vol. 37, pp. 1976–1984, Oct. 1990.

[22] M. M. Hayat, B. E. A. Saleh, and M. C. Teich, "Effect of dead space on gain and noise of double-carrier-multiplication avalanche photodiodes," *IEEE Trans. Electron Devices*, vol. 39, pp. 546–552, Mar. 1992.

[23] M. M. Hayat, W. L. Sargeant, and B. E. A. Saleh, "Effect of dead space on gain and noise in Si and GaAs avalanche photodiodes," *IEEE J. Quantum Electron.*, vol. 28, pp. 1360–1365, 1992.

[24] M. M. Hayat, Z. Chen, and M. A. Karim, "An analytical approximation for the excess noise factor of avalanche photodiodes with dead space," *IEEE Electron Device Lett.*, vol. 20, pp. 344–347, June 1999.

[25] A. Spinelli, A. Pacelli, and A. L. Lacaita, "Dead space approximation for impact ionization in silicon," *Appl. Phys. Lett.*, vol. 69, pp. 3707–3709, 1996.

[26] R. J. McIntyre, "A new look at impact ionization—Part I: A theory of gain, noise, breakdown probability, and frequency response," *IEEE Trans. Electron Devices*, vol. 46, pp. 1623–1631, Aug. 1999.

[27] X. G. Zheng, X. Sun, S. Wang, P. Yuan, G. S. Kinsey, A. L. Holmes, Jr., B. G. Streetman, and J. C. Campbell, "Multiplication noise of $Al_xGa_{1-x}As$ avalanche photodiodes with high Al concentration and thin multiplication region," *Appl. Phys. Lett.*, vol. 78, pp. 3833–3835, 2001.

[28] S. Wang, R. Sidhu, X. G. Zheng, X. Li, X. Sun, A. L. Holmes, Jr., and J. C. Campbell, "Low-noise avalanche photodiodes with graded impact-ionization-engineered multiplication region," *IEEE Photon. Technol. Lett.*, vol. 13, pp. 1346–1348, 2001.

[29] C. K. Chia, J. P. R. David, S. A. Plimmer, G. J. Rees, R. Grey, and P. N. Robson, "Avalanche multiplication in submicron $Al_xGa_{1-x}As$/GaAs multilayer structures," *J. Appl. Phys.*, vol. 88, pp. 2601–2608, 2000.

[30] M. M. Hayat, O.-H. Kwon, Y. Pan, P. Sotirelis, J. C. Campbell, B. E. A. Saleh, and M. C. Teich, "Gain-bandwidth characteristics of thin avalanche photodiodes," *IEEE Trans. Electron Devices*, vol. 49, pp. 770–781, May 2002.

Majeed M. Hayat (S'89-M'92-SM'00) was born in Kuwait in 1963. He received the B.S. degree (summa cum laude) in electrical engineering from the University of the Pacific, Stockton, CA, in 1985, and the M.S. degree in electrical engineering and the Ph.D. degree in computer engineering from the University of Wisconsin-Madison in 1988 and 1992, respectively.

From 1993 to 1996, he was at the University of Wisconsin-Madison as a Research Associate and Co-Principal Investigator of a project on statistical minefield modeling and detection, which was funded by the Office of Naval Research. In 1996, he joined the faculty of the Electro-Optics Graduate Program and the Department of Electrical and Computer Engineering at the University of Dayton, Dayton, OH. He is currently an Associate Professor in the Department of Electrical and Computer Engineering at the University of New Mexico, Albuquerque. His research interests include modeling and design of high-performance photodetectors, optical communication systems, statistical communication theory, communication networks, infrared imaging and sensors, and statistical signal and image processing.

Dr. Hayat is a member of SPIE and the Optical Society of America. He was the recipient of a 1998 National Science Foundation Early Faculty Career Award.
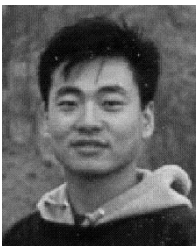
Oh-Hyun Kwon was born in Seoul, Korea, in 1968. He received the B.S. degree in physics from the University of the Hawaii, Manoa, in 1995, and the M.S. degree in electro-optics from the University of Dayton, Dayton, OH, in 1999. He is currently pursuing the Ph.D. degree in electrical and computer engineering at the University of New Mexico, Albuquerque. His research interests include modeling and fabrication of optoelectronic devices, with emphasis on APDs and quantum-dot IR detectors.
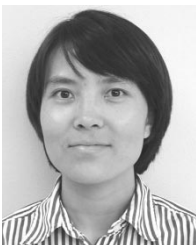
Shuling Wang received the B.S. degree in microelectronics from Beijing University, Beijing, China, in 1995, the M.S.E.E. degree from the University of Notre Dame, Notre Dame, IN, in 1999, and the Ph.D. degree from the University of Texas at Austin in 2002, where she is currently a Postdoctoral Fellow at the Microelectronics Research Center. She is working on high-speed, low-noise avalanche photodiodes.

Joe C. Campbell (S'73–M'74–SM'88–F'90) received the B.S. degree in physics from the University of Texas at Austin in 1969, and the M.S. and Ph.D. degrees in physics from the University of Illinois at Urbana-Champaign in 1971 and 1973, respectively.

From 1974 to 1976, he was with Texas Instruments, where he worked on integrated optics. In 1976, he joined the staff of AT&T Bell Laboratories, Holmdel, NJ. In the Crawford Hill Laboratory, he worked on a variety of optoelectronic devices including semiconductor lasers, optical modulators, waveguide switches, photonic integrated circuits, and photodetectors with emphasis on high-speed APDs for high-bit-rate lightwave systems. In January 1989, he joined the faculty of the University of Texas at Austin as Professor of Electrical and Computer Engineering and Cockrell Family Regents Chair in Engineering. Currently, he is actively involved in Si-based optoelectronics, high-speed APDs, GaN ultraviolet photodetectors, and quantum-dot IR imaging. He has coauthored six book chapters, more than 260 journal publications, and 160 conference presentations.

Dr. Campbell is a Fellow of the Optical Society of America. In 1985, he was recognized by AT&T as Distinguished Member of Technical Staff. In 2002, he was elected into the National Academy of Engineering.

Bahaa E. A. Saleh (M'73–SM'86–F'91) received the B.S. degree from Cairo University, Cairo, Egypt, in 1966, and the Ph.D. degree from Johns Hopkins University, Baltimore, MD, in 1971, both in electrical engineering.

Since 1994, he has been Professor and Chairman of the Department of Electrical and Computer Engineering at Boston University, Boston, MA. He is Deputy Director of the NSF Center for Subsurface Sensing and Imaging Systems, an NSF Engineering Research Center. He is also Co-Director of the Quantum Imaging Laboratory and a member of the Boston University Photonics Center. He held faculty and research positions at the University of Santa Catarina in Brazil, Kuwait University, Max Planck Institute in Germany, the University of California-Berkeley, the European Molecular Biology Laboratory, Columbia University, and the University of Wisconsin-Madison, where he was a faculty member from 1977 to 1994, and served as Chairman of the Department of Electrical and Computer Engineering from 1990 to 1994. His research contributions cover a broad spectrum of topics in optics and photonics including statistical and quantum optics, optical communication and signal processing, nonlinear optics, photodetectors, digital image processing, and vision. He is the author of two books, *Photoelectron Statistics* (New York: Springer-Verlag, 1978) and *Fundamentals of Photonics* (New York: Wiley-InterScience, 1991, with M. C. Teich), chapters in seven books, and more than 180 papers in technical journals. He served as Editor-in-Chief of the *Journal of the Optical Society of America A* from 1991 to 1997, and is presently the Chairman of the Board of Editors of the Optical Society of America.

Dr. Saleh is a Fellow of the Optical Society of America and the Guggenheim Foundation. He is the recipient of the 1999 Optical Society of America Esther Hoffman Beller Award for outstanding contributions to optical science and engineering education. He is also a member of Phi Beta Kappa, Sigma Xi, and Tau Beta Pi.

Malvin C. Teich (S'62–M'66–SM'72–F'89) received the B.S. degree in physics from the Massachusetts Institute of Technology, Cambridge, the M.S. degree in electrical engineering from Stanford University, Stanford, CA, and the Ph.D. degree from Cornell University, Ithaca, NY.

His first professional association was with MIT Lincoln Laboratory, Cambridge, in 1966. He joined the faculty at Columbia University in 1967, where he served as a member of the Department of Electrical Engineering (as Chairman from 1978 to 1980), the Department of Applied Physics, and the Columbia Radiation Laboratory. During his tenure at Columbia, he carried out extensive research in the areas of noise in APDs and fiber-optic amplifiers, photon statistics and point processes, and the generation of squeezed light. In 1996, he was appointed Professor Emeritus of Engineering Science and Applied Physics at Columbia University. Since 1995, he has been teaching and pursuing his research interests at Boston University, Boston, MA, as a faculty member with joint appointments in the Departments of Electrical and Computer Engineering, Physics, and Biomedical Engineering. He is a member of the Quantum Imaging Laboratory, the Photonics Center, and the Center for Adaptive Systems. He also serves as a Consultant to government and private industry. He is most widely known for his work in photonics and quantum optics. His current efforts in photonics are associated with the reduction of noise in APDs and fiber-optic amplifiers; his efforts in quantum optics are directed toward developing imaging systems that make use of the correlation properties of entangled photon pairs generated in nonlinear optical parametric downconversion. He has authored or coauthored approximately 300 technical publications and holds two patents. He is the coauthor of *Fundamentals of Photonics* (New York: Wiley, 1991). He served as a member of the Editorial Advisory Panel for the journal *Optics Letters* from 1977 to 1979, as a member of the Editorial Board of the *Journal of Visual Communication and Image Representation* from 1989 to 1992, and as Deputy Editor of *Quantum Optics* from 1988 to 1994. He is currently a member of the Editorial Board of the journal *Jemná Mechanika a Optika*.

Dr. Teich is a Fellow of the Optical Society of America, the American Physical Society, the American Association for the Advancement of Science, and the Acoustical Society of America. He is a member of Sigma Xi and Tau Beta Pi. He is also a member of the Scientific Board of the Czech Academy of Sciences' Institute of Physics. In 1969, he received the IEEE Browder J. Thompson Memorial Prize for his paper "Infrared Heterodyne Detection." He was awarded a Guggenheim Fellowship in 1973. In 1992, he was honored with the Memorial Gold Medal of Palacký University in the Czech Republic and in 1997, he was the recipient of the IEEE Morris E. Leeds Award. He is currently a member of the Advisory Board of the IEEE Press Series *Emerging Technologies in Biomedical Engineering*.